Plasma-Hydrogenation Effects on Electron Mobility of Laser-Crystallized Poly-Silicon Thin Films for Liquid Crystal Display Panels

Kuninori KITAHARA

Department of Electronic and Control Systems Engineering, Shimane University,
1060 Nishi-Kawatsu, Matsue 690–8504, Japan
(Received September 18, 1998)

Abstract

This paper describes the behavior of H atoms in laser-crystallized poly-Si for thin-film transistors on liquid crystal display panels, where H atoms were penetrated by plasma hydrogenation in order to improve mobility. Mobility was measured by Hall effect. Si-hydrogen bonds were analyzed by Raman scattering. By short-time hydrogenation, penetrated H atoms terminate dangling bonds as the Si–H configuration largely at grain boundaries, which results in the improvement of mobility. By excessive hydrogenation, Si–H_2 bonds are generated simultaneously with degradation of mobility. Si–H_2 bonds are largely formed at in-grain defects. Hydrogenation using the hot-wire method was also made and it was shown that plasma damage does not take a part of those hydrogenation effects. Origin of correlation among Si–H_2, mobility and amount of in-grain defects was discussed based on impurity scattering and weak-bond models.

1. Introduction

Poly-Si on glass substrates has begun to be used for thin-film transistors (TFTs) in liquid crystal display (LCD) panels. Compared to amorphous Si (a-Si) conventionally used for TFT–LCD, poly-Si have larger electron and hole mobilities. The smaller size and improved performance of TFTs are fabricated owing to the higher mobility, which makes LCD suitable for higher definition display applications.

Poly-Si thin films on large-area glass substrates are now prepared by excimer laser irradiation on a-Si film.[1] Dangling bonds at grain boundaries and in-grain defects in poly-Si form deep states and tail states in the bandgap. Hydrogenation of poly-Si is known to passivate dangling bonds resulting in improvement of TFTs characteristics.[2,3] However, the behavior of hydrogen atoms and its effects on electronic properties of poly-Si films are as yet not clear. It might be because most of studies concerning hydrogenation have been made for TFT structures which is not suitable to analyze hydrogen atoms in poly-Si films.

The behavior of hydrogen atoms in Si has been investigated for plasma-deposited a-Si:H and poly-Si with local-vibration modes (LVM) detected by infrared absorption and Raman scattering. The LVM at 2000 cm^{-1} was assigned to Si–H and that at 2100 cm^{-1} was to Si–H_2 or $(Si–H_2)_n (n \geq 2)$.[4,5] In a-Si:H, the dangling bonds are saturated by hydrogen atoms introduced

into the film during preparation.[5] It was mentioned that, in the polycrystalline phase, higher hydrides at 2100 cm^{-1} are dominant and reside most likely at the grain boundaries.[6] Hydrides have been also investigated for single crystalline Si. For the Si surface exposed to CF_4/H_2 reactive ion, it has been shown that the penetrated hydrogen atoms are bounded to the Si lattice and give rise to the Si–H and Si–H_2 vibration modes.[7] In the case of bulk Si treated with hydrogen remote plasma, LVM at 2100 cm^{-1} was assigned as Si–H stretching in platelets.[8]

For laser-crystallized poly-Si thin films used for TFT–LCD, we have found the correlation between the electron mobility and types of hydrides after plasma hydrogenation.[9] However, the origin to obtain the correlation and roles of plasma damage and/or defects in poly-Si remain poorly clarified.

In this work, we report on three subjects. The first subject is the relationship between mobility and types of hydrides generated by plasma hydrogenation. The variation of mobility with generation and dissociation of different types of hydrides is examined. The second subject is influence of plasma damage on that relationship. The relationship between mobility and types of hydrides is also examined for hydrogenation using hot-wire method. The results of hydrogenation with and without plasma are compared. The third subject is implication of grain boundary and in-grain defects in generation of hydrides. In-grain defects are eliminated by high temperature annealing of poly-Si films. Then the mobility and types of hydrides after plasma hydrogenation are examined. Finally, we discuss the mechanism of correlation among the generation of Si–H_2, an amount of in-grain defects and degradation of mobility.

2. Experimental

Procedures of sample preparation and characterization are exhibited in Fig. 1. Unintentionally doped 50-nm-thick a-Si films were deposited on a SiO_2 film on fused quartz substrates using plasma-enhanced chemical-vapor deposition (PECVD). The deposited a-Si films were

PECVD a-Si (50 nm)/SiO$_2$/quartz

↓

Excimer-laser crystallization

↓

P-ion doping

Preanenaling	**600°C**	**1000°C**
Hydrogenation	**Plasma**	**W-hot wire**
Postannealing	**250-550°C**	

Mobility
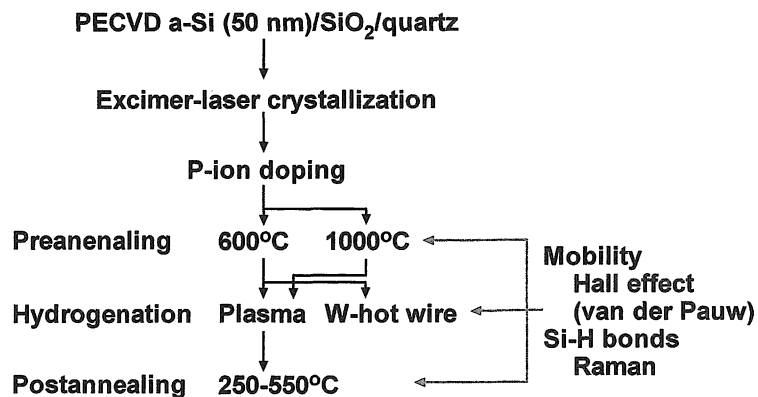**Hall effect**
(van der Pauw)
Si-H bonds
Raman

Fig. 1 Procedures of sample preparation and characterization.

heated to degas the hydrogen. Line-shaped XeCl-excimer laser was irradiated to crystallize a-Si films. The energy density of laser was $\sim$290 mJ/cm^2 and overlapping of pulsed-laser scan was $\sim$90%. Then, phosphorous ions were doped with a dose of 5×10^{13} cm^{-2} to generate free carriers for the measurement of the Hall effect. Films were annealed at 600°C for 2 min in N$_2$ atmosphere to activate doped phosphorous donors. A few samples were annealed at 1000°C for 3 to 360 min in order to examine the effect of the in-grain defects elimination. We refer to annealing at this step as "preannealing". Two methods schematically shown in Fig. 2 were used for hydrogenation. One of them is plasma hydrogenation and the other is hot-wire method. After plasma hydrogenation, some samples were annealed at 250 to 550°C in N$_2$ to examine the effect of hydrogen dissociation. We refer to annealing at this step as "postannealing".

Plasma hydrogenation was performed in the PECVD reactor at 350°C for 1 to 10 min with a radio frequency power of 30 W under the H$_2$ pressure of 300 mTorr. For the hydrogenation without plasma, a tungsten filament was used to generate atomic hydrogen.[10,11] The filament and samples were put in a quartz tube surrounded by a furnace. The filament temperature was 1300°C and pressure of H$_2$ was 1 Torr.

Mobility of poly-Si thin films has been usually measured as field effect mobility of TFTs. However in this work, we measured Hall mobility of electron, μ_0, using van der Pauw technique. The Hall effect measurement is convenient to prepare many samples and to compare electronic properties and types of hydrides detected by optical methods. Apparent free carrier density, n, shown in this work was estimated with neglecting depletion layers at the surface, interface and grain boundaries. Type of hydrides was analyzed with LVM in Raman spectra. Procedures of Raman spectroscopy were described elsewhere.[12] The LVM at 2000 cm^{-1} was dealt as Si–H and that at 2100 cm^{-1} as Si–H$_2$ referring to the assignment for plasma-deposited a-Si and poly-Si.[4-6] The difference between Si-H$_2$ and (Si–H$_2$)$_n$ was not dealt in this work. The sensitivity and frequency of spectrometer were calibrated with the optic phonon mode of strain free single-crystal Si. The intensity of Raman spectra was represented by peak heights instead of peak area be-
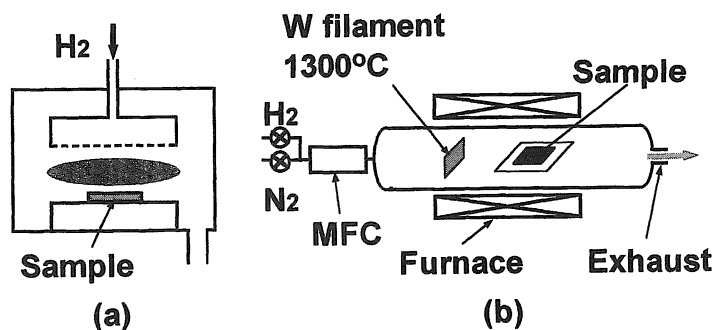

Fig. 2 Setup for hydrogenation of poly-Si. Atomic hydrogen was generated from H$_2$ by using (a) the apparatus for PECVD and (b) a tungsten filament as the hot-wire catalyzer in a quartz tube evacuated to 0.1 Torr.

cause individual peaks were not clearly resolved enough for drawing curve that fits the calculated spectra. Although molecular hydrogen, H_2, can be included in poly-Si layers, its LVM intensity at 4200 cm^{-1} was less than the detection limit of present setup.

3. Results and discussion

3.1 Plasma hydrogenation

For the case of plasma hydrogenation, mobility of poly-Si was plotted as a function of hydrogenation time in Fig. 3. At the step before hydrogenation, mobility is as small as 1.3 cm^2/Vs and n is 1.2×10^{17} cm^{-3}. After 1 min of hydrogenation, mobility increases to 20 cm^2/Vs and n to 1.6×10^{18} cm^{-3}. However, mobility begins to decrease with longer time of hydrogenation, 3 and 10 min. Although the mobility of poly-Si is usually sensitive to n,[13] the present mobility decrement is not attributed to the variation of n because n remains nearly constant for the hydrogenation time of 1 to 10 min. Figure 4 shows the Raman spectra of poly-Si films after hydrogenation. In the case of 1 min hydrogenation, the Si–H peak is dominant (labeled a). After 10-min hydrogenation, Si–H$_2$ peak pronouncedly arises although intensity of Si–H simultaneously increases (labeled b). This suggests that mobility increases with the generation of Si–H. It is also suggested that excessive hydrogenation leads to both the degradation of mobility and the generation of Si–H$_2$.

The penetration of H atoms into poly-Si films by hydrogenation is confirmed by secondary
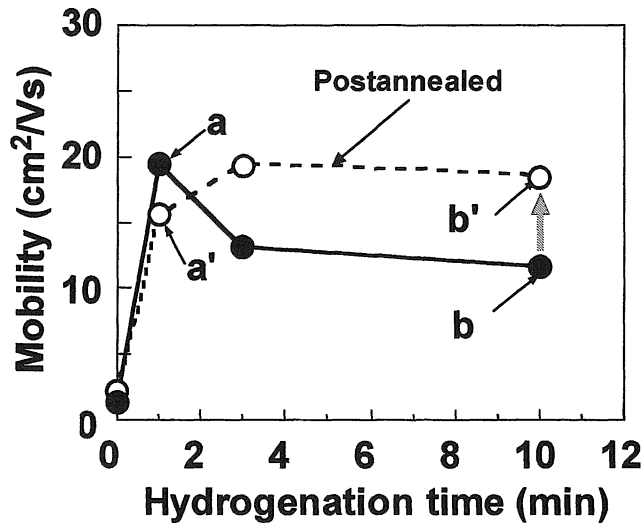

Fig. 3   Dependence of electron mobility on plasma-hydrogenation time, where poly-Si films were annealed at $T_{pre} = 600°C$ to activate doped phosphorus prior to hydrogenation. The broken line shows mobility after post annealing at $T_{post} = 450°C$ for 5 min. Raman spectra for samples labeled a, a′, b and b′ will be shown in Fig. 4.
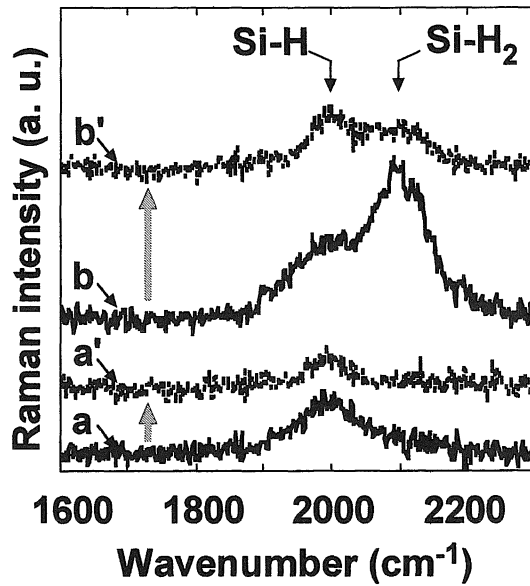
Fig. 4 Raman spectra related to Si-hydrogen bonding stretching modes of poly-Si films plasma
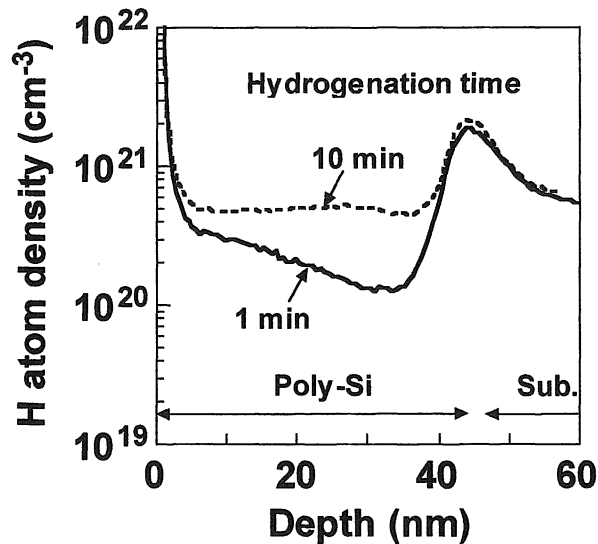hydrogenated for 1 and 10 min. Labels a, a', b and b' correspond to those in Fig. 2.

Fig. 5 Profiles of hydrogen-atom density in poly-Si films hydrogenated with plasma for 1 and 10 min.
Measurement was made by using SIMS.

ion mass spectrometry (SIMS) as shown in Fig. 5. Mean values of H density besides surface and interface regions are 2×10^{20} cm^{-3} for 1 min hydrogenation and 5×10^{20} cm^{-3} (corresponding to 1 at.%) for 10 min hydrogenation. These profiles indicate that trap sites of H atoms are filled from the surface to the bottom of the poly-Si layer with the progress of hydrogenation.

It is expected that excessive H atoms in poly-Si can be dissociated by postannealing. Mobilities of poly-Si films annealed at temperature, T_{post}, of 450°C for 5 min are plotted in Fig. 3. The mobility after 3 or 10-min hydrogenation is improved by postannealing while that after 1-min hydrogenation is slightly decreased. Raman spectra in Fig. 4 indicate that both the Si–H and Si–H$_2$ bonds are eliminated by postannealing. In the case of 1 min hydrogenation, the dominant Si–H peak is weaken by postannealing (labeled a'). In the case of 10-min hydrogenation, Si–H$_2$ bonds are released much than Si–H. Consequently, Si–H regains its dominance in the spectrum (Labeled b'). Therefore, it is deduced that the elimination of Si–H relates to decrease in mobility and that of Si–H$_2$ to increase in mobility.

The effect of postannealing was examined in more detail. The relationship between mobility and T_{post} was plotted in Fig. 6. The mobility increases with rising temperatures and reaches a maximum of 19 cm^2/Vs at T_{post}=450°C. Then the mobility begins to decrease and reaches a value as small as that before hydrogenation. This temperature dependence of mobility is understood by the difference between the dissociation energies of Si–H and Si–H$_2$, where the energy for Si–H$_2$ is less than that for Si–H.[14] Thus, Si–H$_2$ begins to dissociate at lower temperature than Si–H resulting in increase in mobility at $T_{post} \leq$450°C. Above 450°C, Si–H continues to actively dissociate resulting in decrease in mobility.
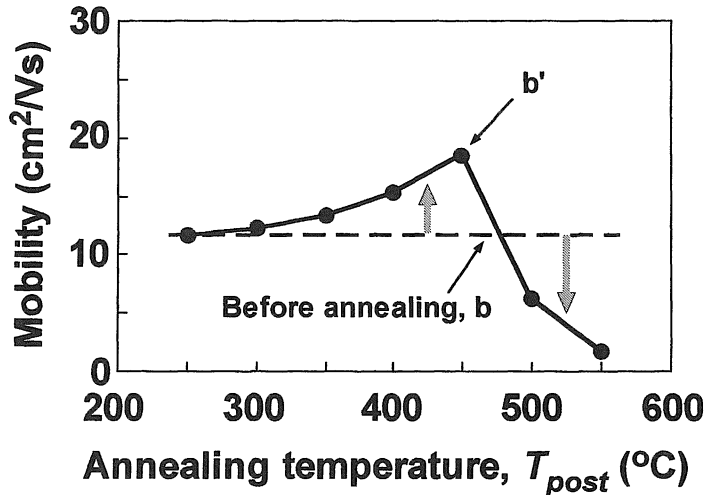

Fig. 6   Relationship between the mobility of excessively hydrogenated (10 min) samples and temperature of postannealing after this hydrogenation, T_{post}. The broken line demonstrates the mobility before postannealing. Labels b and b' correspond to those in Figs. 2 and 3.

Therefore, the variations of mobility with hydrogenation and postannealing are related to the generation and dissociation of hydrides as follows; (1) the generation of Si–H relates to the increase in mobility; (2) excessive hydrogenation causes both degradation of mobility and generation of Si–H$_2$; (3) dissociation of Si–H results in the decrease in mobility; (4) dissociation of Si–H$_2$ causes recovery of mobility. It should be noted that the relationships of (1) and (2) are consistent with those of (3) and (4), respectively.

3.2 Hydrogenation with hot-wire method

Figure 7 shows the relationship between mobility and hydrogenation time in the case of the hot-wire method. The temperature of the furnace surrounding the reactor tube was set to 300°C and the distance from the hot wire to specimen, L, was to 100 mm. The sample temperature, T_s, measured at its holder is 326°C, which is higher than that of the furnace because of the radiant heat from the hot wire. The mobility drastically arises with hydrogenation. However, it begins to decrease at time longer than 180 min. This time dependence of the mobility is similar to that for plasma hydrogenation while the scale of time is far larger. The pronounced decrease in mobility (labeled II) is caused by drawing sample to hot wire, where L is 40 mm. In this case, T_s rises to 374°C due to the radiant heat.

Figure 8 shows the Raman spectra of poly-Si films corresponding to labels I and II in Fig. 7. In the case of $L=100$ mm (labeled I), Si–H is dominant. In the case of $L=40$ mm (labeled II), the Si–H$_2$ peak become to be intensive and dominant while the of Si–H peak simultaneously arises. Thus, the pronounced decrease in the mobility (labeled II in Fig. 7) is attributed
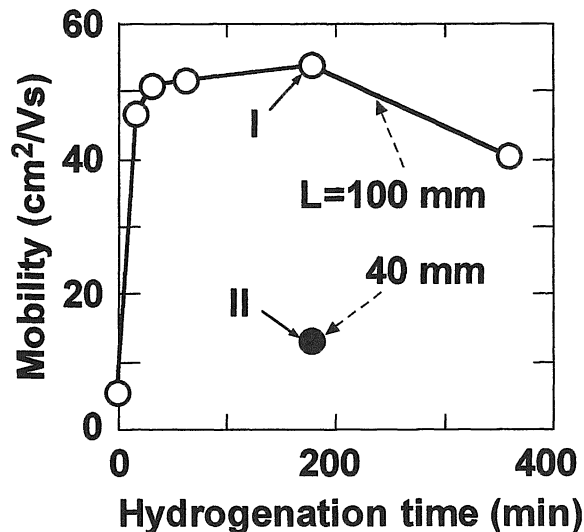

Fig. 7   Dependence of mobility on times of hydrogenation using hot-wire method. Distance between specimens and hot wore L is 100 mm (open circles) or 40 mm (closed circle).
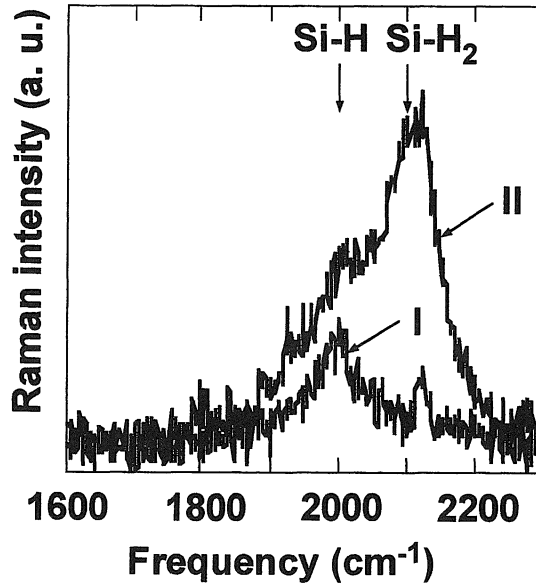
Fig. 8   Raman spectra after hydrogenation for 180 min by hot-wire method. Labels I and II correspond to those in Fig. 7.

rather to the enhancement of hydrogenation followed by the Si–H_2 generation than to thermal dissociation of Si–H due to rising T_s.

Based on Figs. 7 and 8, the generation of Si–H is related to the increment of mobility and that of Si–H_2 is to the decrement of mobility. This relationship is the same as those for plasma hydrogenation. Therefore, plasma damage does not take part in the relationship among mobility, type of hydrides and hydrogenation time. Furthermore, it is deduced that amount of penetrated hydrogen atoms determines the type of hydrides and mobility.

3.3   Roles of grain boundaries and in-grain defects

Both of the Si–H and Si–H_2 bonds should be formed by termination of dangling bonds at imperfections such as grain boundaries and in-grain defects. Annealing of poly-Si at T_{pre} = 1000°C prior to hydrogenation seems to be useful to distinguish contributions of grain boundaries and in-grain defects because it was expected that in-grain defects are eliminated at this temperature while the grain size is unchanged. Figure 9 shows images of plan-view transmission electron microscopy (TEM) of the poly-Si films annealed at T_{pre} = 600°C for 2 min and at T_{pre} = 1000°C for 10 min. The procedure of 600°C annealing is the same as one used to activate phosphorus donor atoms. TEM images exhibit that the amount of in-grain defects was apparently reduced by rising T_{pre} while the mean grain size of 80 nm was unchanged, where most of in-grain defects revealed are stacking faults.

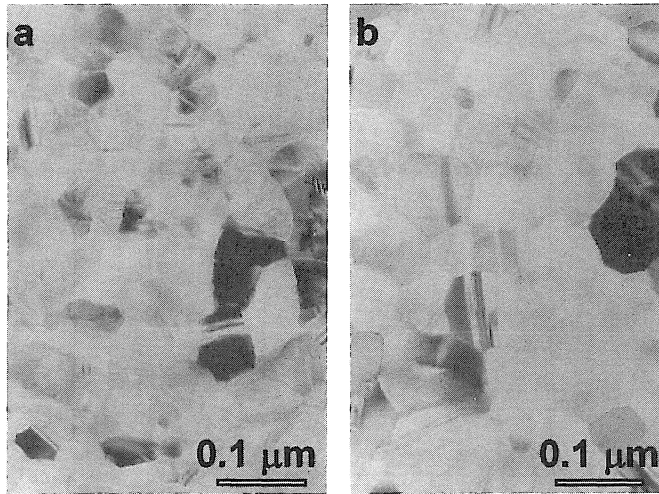Figure 10 shows relationship between mobility and plasma-hydrogenation time for poly-Si

Fig. 9   Plan-view TEM images of poly-Si films annealed at (a) $T_{pre}=600°C$ for 2 min and (b) T_{pre}
=1000°C for 10 min. In-grain defects were eliminated at the higher temperature although grain
size remained constant.
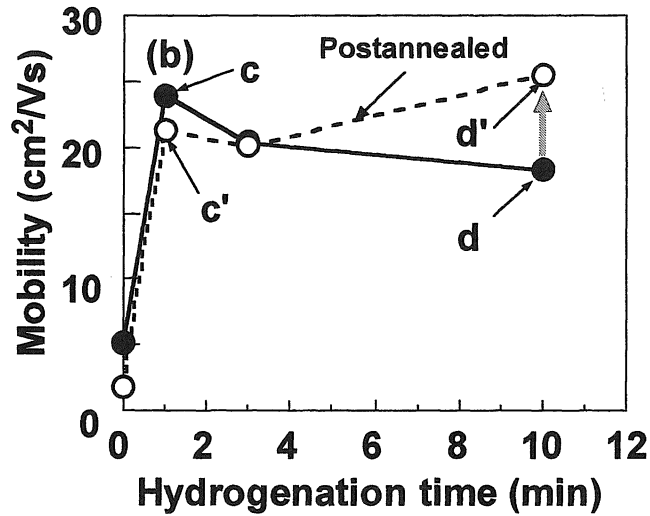

Fig. 10   Dependence of electron mobility on plasma hydrogenation time, where poly-Si films were prean-
nealed at $T_{pre}=1000°C$ to eliminate in-grain defects. The broken line shows mobility after post an-
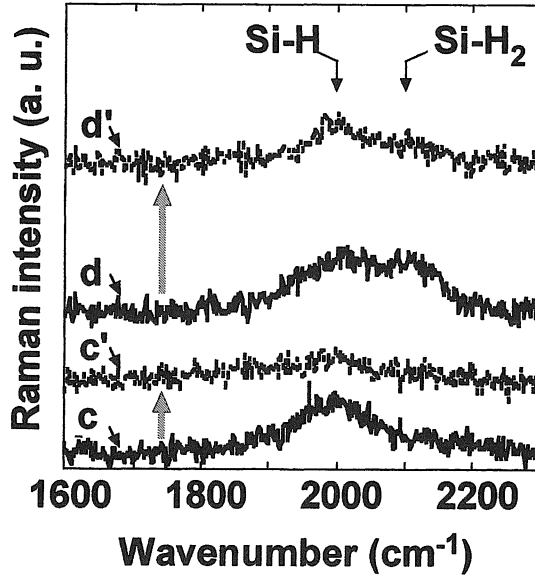nealing at $T_{post}=450°C$ for 5 min. Raman spectra for samples labeled c, c′, d and d′ will be shown
in Fig. 11.

Fig. 11   Raman spectra related to Si-hydrogen bonds for samples plasma hydrogenated for 1 and 10 min after preannealing at $T_{pre}=1000°C$. Labels c, c', d and d' correspond to those in Fig. 10.

films annealed at $T_{pre}=1000°C$. Raman spectra of some of these films are also shown in Fig. 11. In the case of 1-min hydrogenation, the mobility is significantly increases, and the Si–H peak is dominant in spectrum (labeled c). By extending hydrogenation time to 10 min, the mobility is degraded, and Si–H$_2$ peak arises (labeled d). The degraded mobility is recovered by post annealing at 450°C (labeled c'). These relationships between mobility and Raman spectra seen to be nearly the same as those for $T_{pre}=600°C$ shown in Figs. 3 and 4. However, obvious difference appears in Raman spectra, where the peak height of Si–H$_2$ is apparently smaller than that of $T_{pre}=600°C$. Furthermore, ratio of the mobility degradation due to excessive hydrogenation is not so large as $T_{pre}=600°C$ shown in Fig. 3. In Fig. 12, mobility and the intensity ratio of Si–H$_2$ to Si–H peaks, I_{Si-H_2}/I_{Si-H}, are plotted as a function of $T_{pre}=1000°C$-annealing time. With increase in time, the mobility gradually increases and the ratio decreases. This implies that both the generation of Si–H$_2$ and the degradation of mobility caused by excessive hydrogenation closely relate to the amount of in-grain defects. On the contrary, pronounced dependence of the Si–H intensity on preannealing time is not observed. Therefore, it is deduced that Si–H$_2$ is formed largely at in-grain defects and Si–H is at grain boundaries.

3.4   Implications in mobility, types of hydrides and defects

We now discuss the mechanism of implications in mobility, types of hydrides and defects. For Si–H bonds, its effects on mobility can be understood by termination of dangling bonds largely at grain boundaries resulting in elimination of charged states. Release of H atoms from
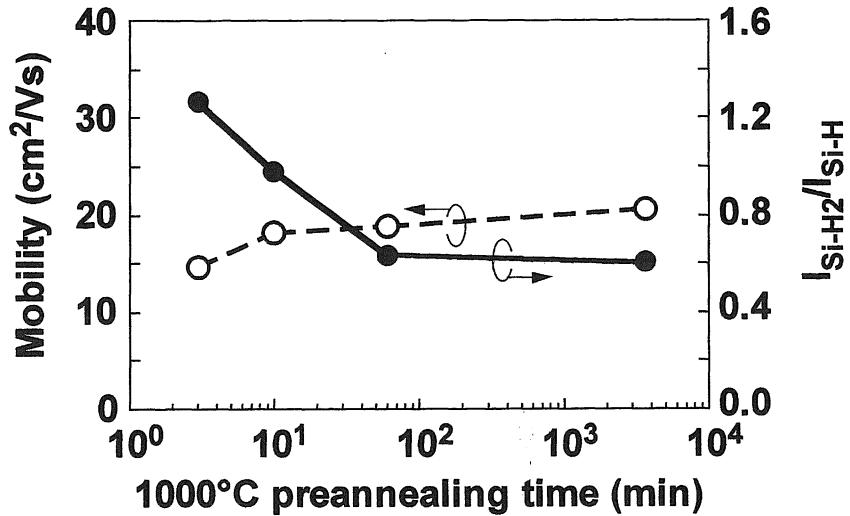
Fig. 12   Mobility and intensity ratio of Raman spectra for Si–H$_2$ to Si–H plotted as a function of time of
preannealing at 1000°C. The samples were plasma-hydrogenated for 10 min after preannealing.

grain boundaries by postannealing reforms dangling bonds leading to degradation of mobility.

For Si–H$_2$ bonds, it is not easy to interpret their correlation with mobility and in-grain defects. Hall mobility of poly-Si is usually determined by density of charged states when n and grain size are constant. However, Si–H$_2$ unlikely form charged states because dangling bonds should be terminated to be neutral. We assumed two models; one is neutral-impurity scattering and the other is conversion from weak-bonds to dangling bonds. Density of hydrogen atoms is so large as 5×10^{20} cm^{-3}. Therefore, amount of Si–H$_2$ can be also large enough to act as an effective scattering center for carries. However, relationship between Si–H$_2$ and in-grain defects cannot be interpreted with this model. Creation of dangling bonds associated with hydrogen has been proposed for light-induced degradation in a-Si:H.[15–17] Conversion from weak bonds to dangling bonds are caused by the motion of H atoms associates to this process.[16] It was mentioned that a-Si films with a high Si–H$_2$ bond density have large structural flexibility because the Si atoms, bonded as Si–H$_2$, is a two-fold coordination.[17] Although in this experiment the material is poly-Si and intentional optical exposure was not made, the Si–Si bonds immediately adjacent to in-grain defects are assumed to be weak. Therefore, the bonds can be broken by the assistance of penetrated H atoms leading to generation of dangling bonds simultaneously with formation of Si–H$_2$ at grain boundaries. These dangling bonds act as charged-scattering centers for mobility. By postannealing, the dangling bonds can be eliminated simultaneously with dissociation of Si–H$_2$ because it is known that photo-induced degradation of a-Si:H was recovered by annealing at temperature as low as 150°C.[15]

4. Summary

    Relationship among mobility, Si-hydrogen bonds and imperfections in plasma-hydrogenated poly-Si thin films was investigated. Two types of hydrides, Si–H and Si–H$_2$, were found with local-vibration modes in Raman spectra. By short-time hydrogenation, penetrated H atoms terminate dangling bonds as the Si–H configuration largely at grain boundaries, which results in the improvement of mobility. By excessive hydrogenation, Si–H$_2$ bonds are generated simultaneously with degradation of mobility. Si–H$_2$ bonds are largely formed at in-grain defects. Dissociation of Si–H and Si–H$_2$ by postannealing respectively leads to decrease and increase in mobility, which is consistent with the effects of hydrides generation. Hydrogenation by using the hot-wire method was also made and it was deduced that plasma damage does not take a part of those hydrogenation effects. Relationship among the generation of Si–H$_2$, decrease in mobility and amount of in-grain defects was discussed in terms of two models; the neutral-impurity scattering, and the weak-bonds to dangling bonds conversion caused by excessive hydrogenation.

References

1) T. Sameshima, S. Usui, and M. Sekiya: IEEE Electron Dev. Lett. **EDL-7** (1986) 276.
2) T. I. Kamins and P. J. Marcoux: IEEE Electron Device Lett. **EDL-1** (1980) 159.
3) I-W. Wu, T-Y. Huang, W. B. Jackson, A. G. Lewis, and A. Chang: IEEE Electron Device Lett. **EDL 12** (1991) 181.
4) G. Lucovsky, R. J. Nemanichi, and J. C. Knights: Phys. Rev. B **19** (1979) 2064.
5) M. H. Brodsky, M. Cardona, and J. J. Cuomo: Phys. Rev. B **16** (1977) 3556.
6) C. C. Tsai: *Amorphous Silicon and Related Materials* (ed. by H. Fritzsche, World Scientific, Singapore, 1988) pp. 125.
7) G. S. Oehrlein, R. N. Tromp, J. C. Tsang, Y. H. Lee, and E. J. Petrillo: J. Electrochem. Soc. **132** (1985) 1441.
8) K. Murakami, N. Fukuta, S. Sasaki, K. Ishioka, M. Kitajima, S. Fujimura, J. Kikuchi, and H. Haneda: Phys. Rev. Lett. **77** (1996) 3161.
9) K. Kitahara, S. Murakami, A. Hara, and K. Nakajima, Appl. Phys. Lett. **72** (1998) 2436.
10) I. Langmuir: J. Am. Chem. Soc. **36** (1914) 417.
11) R. Ishihara and M. Matsumura: Jpn. J. App. Phys. **36** (1997) 6167.
12) K. Kitahara, K. Suga, A. Hara and K. Nakajima: Jpn. J. Appl. Phys. **35** (1996) L1473.
13) J. Y. W. Seto: J. Appl. Phys. **46** (1975) 5247.
14) P. Gupta, V. L. Colvin, and S. M. George: Phys. Rev. B **37** (1988) 8234.
15) D. L. Staebler and C. R. Wronski: Appl. Phys. Lett. **31** (1977) 292.
16) R. A. Street and K. Winer: Phys. Rev. B **40** (1989) 6236.
17) N. Nakamura, T. Takahama, M. Isomura, M. Nishikuni, K. Yoshida, S. Tsuda, S. Nakano, M. Ohnishi and Y. Kuwano: Jpn. J. Appl. Phys. **28** (1989) 1762.